Available online at www.sciencedirect.com

ScienceDirect

Ceramics International 42 (2016) 3296–3303

CERAMICS INTERNATIONAL

www.elsevier.com/locate/ceramint

Sintering behavior and microwave dielectric characteristics of $ZnTiNb_2O_8$ ceramics achieved by reaction sintering of $ZnO–TiO_2–Nb_2O_5$ nanosized powders

H. Barzegar Bafrooei[a], E. Taheri Nassaj[a,*], T. Ebadzadeh[b], C.F. Hu[c], A. Sayyadi-Shahraki[a], T. Kolodiazhnyi[d]

[a]Department of Materials Science and Engineering, Tarbiat Modares University, P.O. Box 14115-143, Tehran, Iran
[b]Ceramic Division, Materials and Energy Research Centre, P.O. Box 14155-4777, Alborz, Iran
[c]Key Laboratory of Advanced Technologies of Materials, Ministry of Education, School of Materials Science and Engineering, Southwest Jiaotong University, Chengdu, Sichuan 610031, China
[d]National Institute for Materials Science, 1-1 Namiki, Tsukuba, Ibaraki 305-0044, Japan

Received 1 June 2015; received in revised form 19 September 2015; accepted 23 October 2015
Available online 31 October 2015

Abstract

Sintering behavior, microstructure and microwave dielectric properties of $ZnTiNb_2O_8$ (ZTN) ceramics prepared by reaction-sintering method were investigated. The prepared ceramic samples were characterized by field emission scanning electron microscopy, X-ray diffraction, and microwave dielectric measurements. All samples prepared at sintering temperatures ranging from 1025 to 1125 °C exhibit a single ixiolite phase and their relative densities range from ~86.5 % to ~99 %. The variation trend of permittivity and $Q \times f$ value was in accordance with variation trend of relative density. Pure ixiolite ZTN ceramic sintered at 1075 °C for 5 h exhibits good microwave dielectric properties with a permittivity about 36.7, $Q \times f$ value about 54,000 GHz, and temperature coefficient of resonant frequency about −70.4 ppm/°C. The obtained results demonstrated that the reaction-sintering process is a simple and effective method to prepare the $ZnTiNb_2O_8$ ceramics for passive microwave dielectric devises.

Keywords: Reaction sintering; Microwave dielectric ceramic; $ZnTiNb_2O_8$

1. Introduction

As the key basic materials for the modern communication technology, microwave dielectric ceramics are widely used as a filters for mobile communication equipment, base stations for cell phones, microwave transmitting circuit for receiving satellite broadcasting, GPS antenna, Bluetooth, and recently for ITS (Intelligent Transportation System) [1–3]. In order to meet the specifications of current and future systems, improved or new microwave components based on the dedicated dielectric materials are required.

Among several kinds of dielectric ceramics, ixiolite $ZnTiNb_2O_8$ (ZTN) becomes a well-known material for low cost resonators, filters and antennas operating at millimeter-wave frequencies due to the high quality factors and appropriate dielectric constant. Until now much attention was paid to research on microwave dielectric properties of ceramics prepared by the conventional solid-state method [4–10]. For instance, the sintering temperature of ZTN ceramics was firstly reported to be about 1250 °C with a dielectric constant of 34, $Q \times f$ of 42,500 GHz and τ_f of −52 ppm/°C by Kim et al [4,5]. Liao and Li [9] reported that the ZTN precursor was synthesized at 900 °C for 3 h and then sintered at 1120 °C for 6 h with dielectric constant $\varepsilon = 34.4$, $Q \times f = 56{,}900$ GHz, $\tau_f = -47.94$ ppm/°C. In addition, Lei et al [10] also reported that the ZTN

*Corresponding author.
E-mail address: taheri@modares.ac.ir (E.T. Nassaj).

http://dx.doi.org/10.1016/j.ceramint.2015.10.121
0272-8842/

powders could be obtained at 1050 °C via traditional solid-state method and $ZnTiNb_2O_8$ sintered at 1150 °C exhibited the best microwave properties: high permittivity ($\varepsilon_r = 34.2$), high quality factor ($Q \times f = 28{,}696$ GHz), but large negative temperature coefficient of the resonant frequency ($\tau_f = -75.841$ ppm/°C). Recently, Mei et al [11] reported that the ZTN powders could be obtained at 700 °C via an aqueous sol–gel process. They obtained a dielectric constant $\varepsilon_r = 35.3$, quality factor $Q \times f = 66{,}700$ GHz, and $\tau f = -55.4$ ppm/°C for ZTN ceramics sintered at 1050 °C for 2 h.

Reaction-sintering process is a simple and effective method to obtain ceramics with high relative density. In this process, the mixture of raw materials is pressed and sintered directly without any calcination and subsequent ball-milling stages involved in the conventional solid state process. The reactions between raw materials take place during sintering process at high temperatures. The major difference between reaction-sintering process and conventional solid state process is that the particles in the compact pellets prior to sintering are not highly agglomerated clusters as those in the calcined or high-energy milled powders [12]. Therefore, the reaction-sintering process can enhance densification progress. Liou and co-workers reported microwave dielectric ceramics such as $BaTi_4O_9$, $(Ba_xSr_{1-x})(Zn_{1/3}Nb_{2/3})O_3$, $(Pb,Ca)(Fe_{0.5}Nb_{0.5})_{1-x}Ti_xO_3$, $Ba_5Nb_4O_{15}$, $Sr_5Nb_4O_{15}$, $CaNb_2O_6$, $ZnNb_2O_6$, $MgTiO_3$–$MgTi_2O_5$, $BiNbO_4$, $Ni_4Nb_2O_9$ and $MgAl_2O_4$–$CoAl_2O_4$ using reaction sintering process [13–22].

Recently, our group reported sintering behavior and microwave dielectric characteristics of $ZnNb_2O_6$ and $Li_2ZnTi_3O_8$ ceramics obtained by reaction sintering [12,23]. Although ZTN ceramic has been studied by several researchers, the reports on the preparation of ZTN ceramic by the reaction-sintering method are not readily available. In the present work, ZTN ceramics were prepared using reaction-sintering process. Phase composition, densification, microstructure and microwave dielectric properties of the ceramics were investigated.

2. Exprimental procedure

Highly pure powders of ZnO, TiO_2 and Nb_2O_5 (all from Sigma Aldrich Co, USA) were mixed in stoichiometric proportions to form $ZnTiNb_2O_8$. The milling was carried out with high-energy planetary mill. A WC vial with a diameter of 80 mm and 60 WC balls with diameter of 10 mm were used as the milling medium. The required amount of powder mixture for 15:1:1 ball to powder to ethanol mass ratio (BPMR) was used. The raw materials were milled in air at room temperature for 20 h. The rotation speed of the disk was 210 rpm and that of the vials was 525 rpm. After the slurry was dried and admixed with 5 wt% polyvinyl alcohol (Aldrich) as a binder, the as-obtained powder was pressed at 150 MPa into disk-shaped pellets of 10 mm diameter and 5 mm thickness. These pellets were then sintered at 1025–1125 °C for 1–5 h in air on alumina plate.

The density of sintered pellets was measured using the Archimedes method. The sintered pellets were analyzed by powder X-ray diffraction (XRD) to check the phase purity using CuK_α radiation (XRD, Bruker AXS D8 Discover, Germany). Microstructures were analyzed by scanning electron microscopy (SEM, Hitachi S-4800, Japan).

The MW measurements were performed in the frequency range of 6.5–7.5 GHz using the resonant cavity method as described in Ref. [24]. The diameter-to-thickness ratio of the DR was adjusted to ≈ 2.26 to make certain that the first resonance mode is of the $TE_{01\delta}$-type. The DR was placed on top of the low-loss quartz support in the center of the silver-clad cylindrical resonance cavity (QWED, Poland). The microwave resonances in transmission mode (s_{21} parameter) were measured using the HP 8719C vector network analyzer. The dielectric constant was calculated using the QWED software (QWED, Poland) which takes into account the geometry of the DR and the metal enclosure. The unloaded Q-factor was calculated according to:

$$Q = \frac{Q_l}{1 - 10^{-P/20}},$$

where Q_l is the loaded quality factor determined from the full width of the resonance peak at the 3 dB level, and P is the absolute value of the s_{21} parameter at the resonance in dB. Temperature coefficient of the resonance frequency, τ_f, was measured in the temperature interval of +20 to +90 °C and obtained according to:

$$\tau_f = \frac{\Delta f}{f_0 \times \Delta T},$$

where Δf is a shift of the resonant frequency, f_0, introduced by a temperature change of ΔT.

3. Results and discussion

Fig. 1a and b shows the XRD pattern and morphology of the high energy ball milled powders, respectively. Fig. 1a shows the XRD pattern of milled powder consisting mainly of three major crystalline phases of ZnO, TiO_2 and Nb_2O_5 that are similar to the raw powders in phase composition. No ZnTiNb2O8 phase was found in the as-milled powders. It indicates that there were no obvious chemical reactions between ZnO, TiO_2 and Nb_2O_5 during the ball milling process. It can be observed that the milled powders consist of nanopowder agglomerates composed of fine crystallites (Fig. 1b). The specific surface area of the milled powder was determined by Brunauer–Emmett–Teller (BET) technique (Micromeretics Gemini 2360, USA) and found to be 17.4 $m^2\,g^{-1}$.

The XRD patterns of ZTN ceramics sintered at 1025 and 1125 °C for different soaking times are shown in Fig. 2. For all samples only ixiolite phase (JCPD file no. 48-0323) was present, up to the detection limit of the technique. Ixiolite $ZnTiNb_2O_8$ belongs to the orthorhombic crystal system (space group *Pbcn*, no. 60, $a = 4.6746(5)$ Å, $b = 5.6621(5)$ Å, $c = 5.0137(4)$ Å) where Ti, Zn and Nb ions are statistically distributed over the cation sites. The structure is closely related to the columbite $ZnNb_2O_6$ where Zn and Nb cations form an ordered superstructure array to minimize the Nb^{5+}–Nb^{5+}

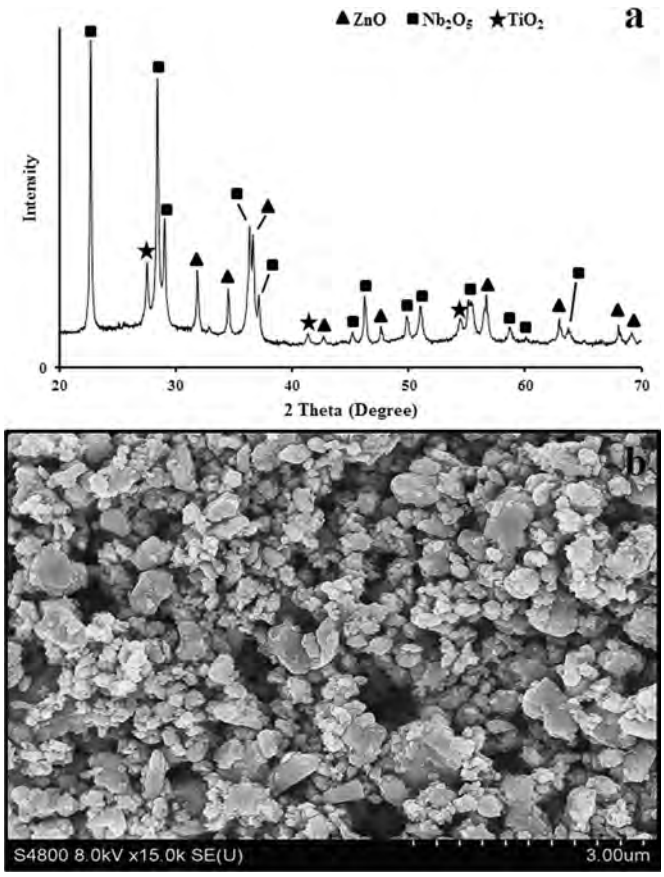

Fig. 1. (a) X-ray diffraction (XRD) pattern and (b) scaning electron microscopy (SEM) micrograph of high energy ball milled ZnO-Nb_2O_5–TiO_2 nanopowders.

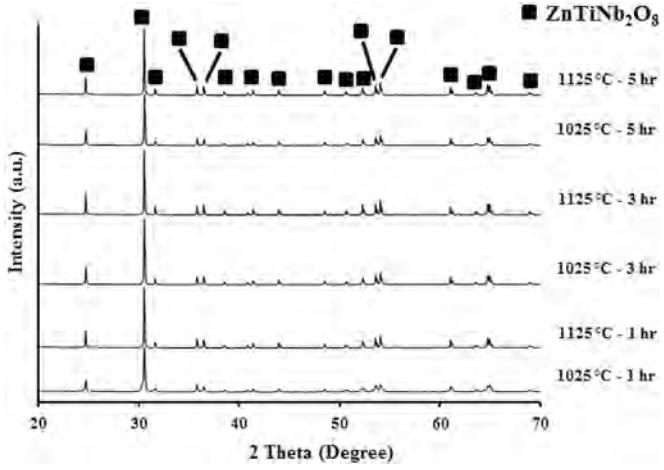

Fig. 2. XRD patterns of ZTN ceramics sintered at 1025 and 1125 °C for, (a) 1 h, (b) 3 h and (c) 5 h.

coulomb repulsion [25]. The ordered arrangement of the Zn and Nb cations in the $ZnNb_2O_6$ columbite results in the tripling of the *a* unit length as compared to the disordered ixiolite. The powder XRD results indicate that the reaction sintering of $ZnTiNb_2O_8$ ceramics is an adequate processing method

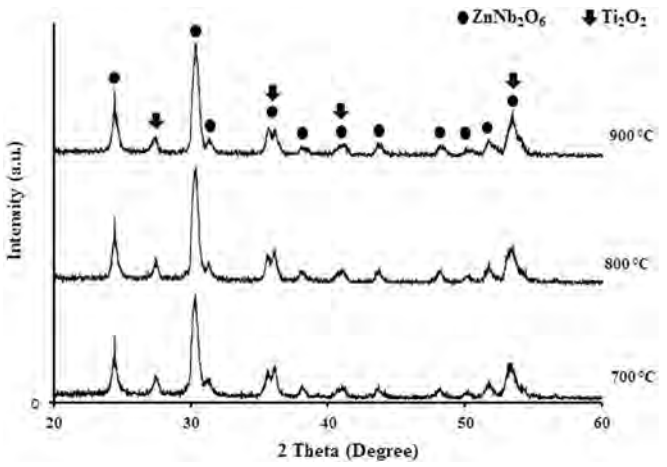

Fig. 3. The XRD patterns of ZnO–TiO_2–Nb_2O_5 nanosized powders were calcined at 700–900 °C for 1 h.

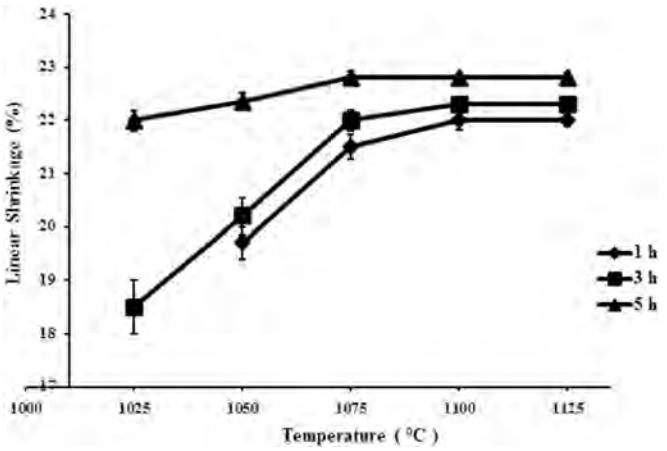

Fig. 4. Shrinkage percentages of ZTN ceramics sintered at various temperatures for 1–5 h.

because the raw materials (ZnO, TiO_2, and Nb_2O_5) were not present at the end of the sintering, although no prior calcination treatment was performed. In addition, the XRD patterns of the ZTN ceramics system have no significant change with sintering temperatures and soaking times in the range of 1025–1125 °C and 1–5 h, respectively. This indicates that the reaction-sintering process is a simple and effective route to produce ZNT ceramics.

Usually, it is necessary to investigate the formation mechanism of the phase composition when trying to prepare a ceramics using Reaction Sintering method, so ZnO–TiO_2–Nb_2O_5 nanosized powders were calcined at 700–900 °C for 1 h and the XRD patterns of these powders are shown in Fig. 3. When the powders were calcined at the low temperature 700 °C, $ZnNb_2O_6$ and TiO_2 phases were formed. The heat treatment at high temperatures (800 °C and 900 °C) only resulted in the increase and decrease of peak intensity of $ZnNb_2O_6$ and TiO_2, respectively. In compare with ceramics sintered in temperature higher than 1000 °C (Fig. 2), $ZnNb_2O_6$ and TiO_2 reacted and resulted in $ZnTiNb_2O_8$. The related

chemical equations are shown in detail below:

$$ZnO + Nb_2O_5 + TiO_2 \xrightarrow{< 1000\ ^\circ C} ZnNb_2O_6 + TiO_2 \quad (1)$$

$$ZnNb_2O_6 + TiO_2 \xrightarrow{> 1000\ ^\circ C} ZnTiNb_2O_8 \quad (2)$$

The shrinkage evolution of the sintered ZNT pellets is illustrated in Fig. 4. The shrinkage increases from 19.7% to 22% at 1025 °C to 22–22.8% at 1125 °C. Longer soak time results in larger shrinkage at low sintering temperatures. It is also observed that after 1, 3 and 5 h soaking the maximum shrinkage occurred at 1100, 1100 and 1075 °C, respectively. Mei et al reported a diametric shrinkage ratio of ~17% for ZTN ceramics obtained by the aqueous sol–gel process and the solid state technique [11].

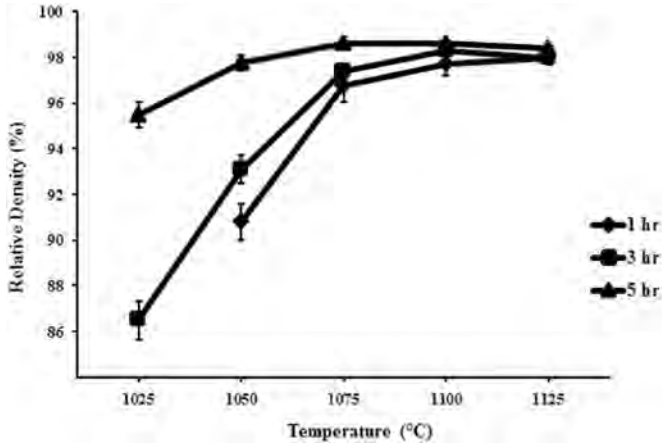

Fig. 5. Density of ZTN ceramics sintered at various temperatures for 1–5 h.

The influence of the sintering temperature and the soaking time on the density of the ZTN ceramics is shown in Fig. 5. The results show similar tendency to that observed for the shrinkage behavior (Fig. 4). The density of the specimens increased with increasing sintering temperature and time. This behavior can be attributed to the decrease in porosity, the grain growth and the formation of the dense microstructures as confirmed by the SEM images shown in Fig. 6–8. A density of 5.27 g/cm^3 (98.6% of the theoretic density) is measured after 5 h sintering at 1075 °C. Park et al. [26] reported a relative density of 97% for ZTN after calcination at 1050 °C for 3 h and sintering at 1250 °C for 2 h. On the other hand, a density of ZTN close to 97% was reported by Zhou et al. [27] by using 3 wt% $BaCu(B_2O_5)$ addition and calcining at 1080 °C for 2 h and sintering at 950 °C for 2 h. Therefore, reaction-sintering process is effective to produce high density ZTN ceramics even without any calcination and the sintering aid.

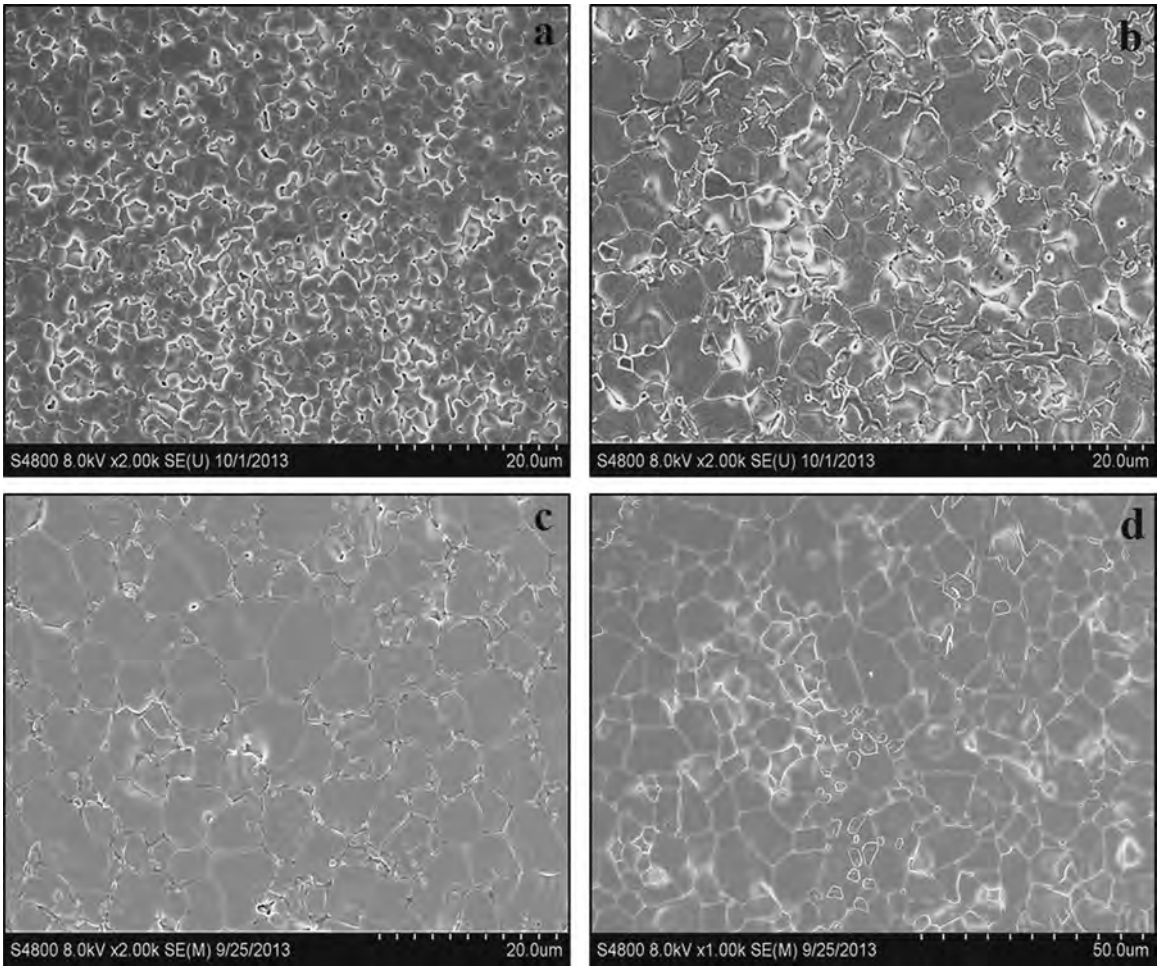

Fig. 6. SEM photographs of ZTN ceramics sintered at different temperatures for 1 h.

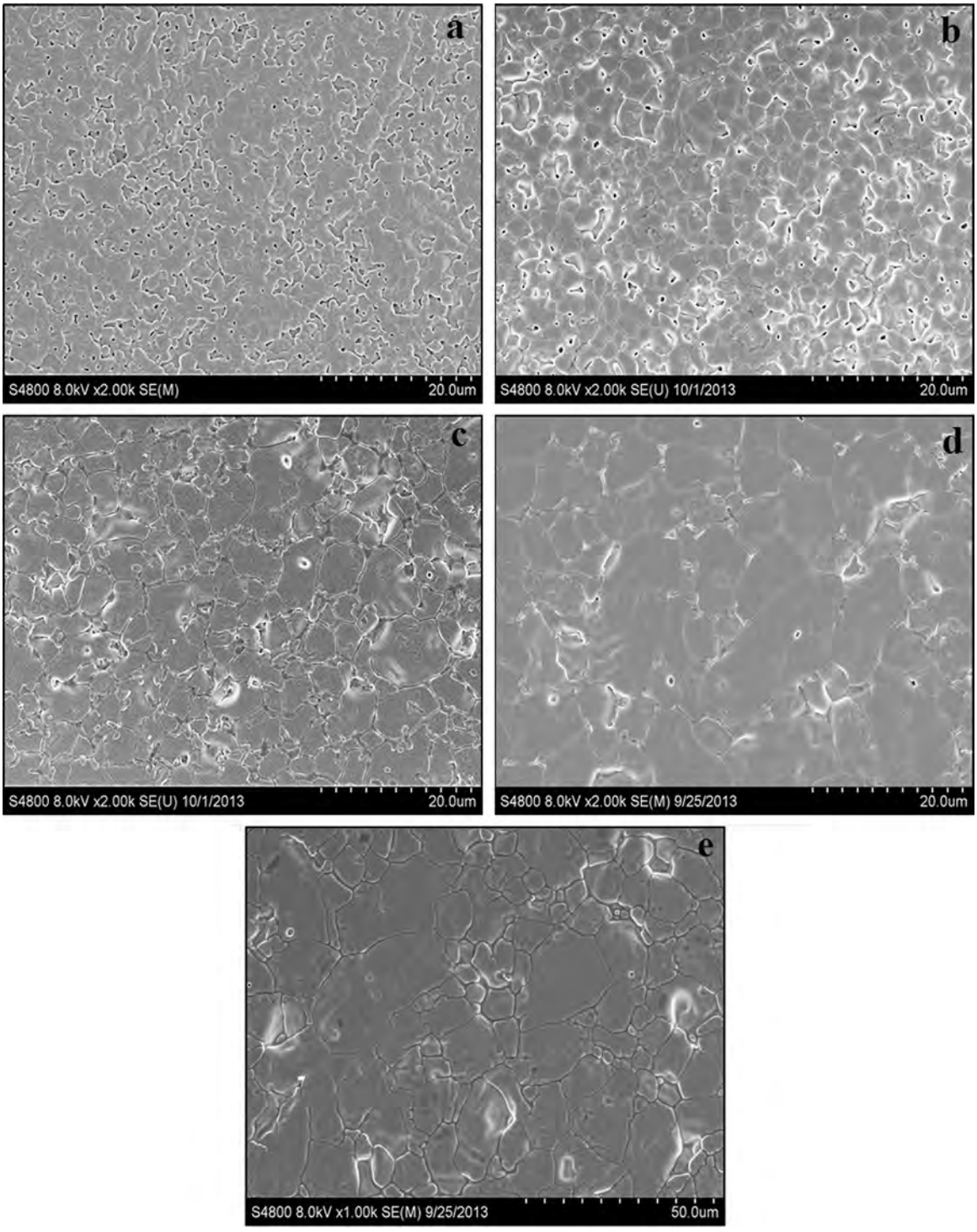

Fig. 7. SEM photographs of ZTN ceramics sintered at different temperatures for 3 h.

The SEM micrographs of ZTN ceramics sintered at 1025–1125 °C for 1 h are shown in Fig. 6. Porous pellets with small grains less than 2 μm are observed in ZTN ceramics sintered at 1025 °C which resulted in a low density of 4.85 g/cm^3. Pores decreased and grain growth increased in pellets sintered at higher sintering temperatures. Grains of larger than 10 μm in size could be found in a high density ZTN ceramic (5.27 g/cm^3) sintered at 1075 °C for 5 h. Almost no pores were observed in the ceramic sintered at 1075°. Pores decreased and larger grains were found in the samples sintered for 3 and 5 h as shown in Figs. 7 and 8. This may explain why the shrinkage and density of the samples sintered for 3 and 5 h are higher than those of samples sintered for 1 h.

Fig. 9 shows the dielectric constant values of ZTN ceramics versus the sintering temperature and time. In the absence of the ferroelectric and Debye-type dipolar contribution, the intrinsic dielectric constant of crystalline ceramics at the microwave frequencies is determined by the sum of the optical phonon

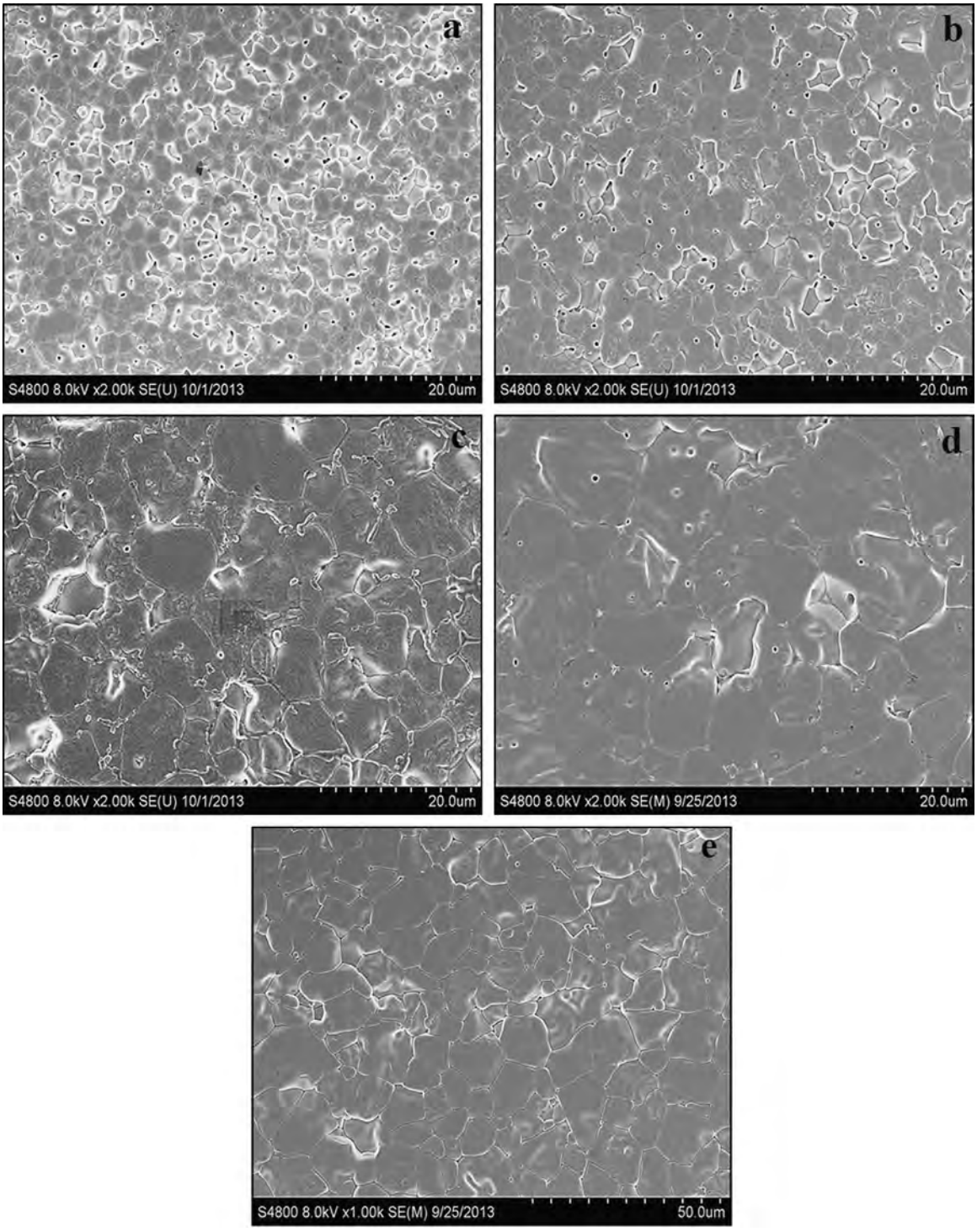

Fig. 8. SEM photographs of ZTN ceramics sintered at different temperatures for 5 h.

contribution, ε_{ph}, and the electron contribution, ε_e, the latter term being much smaller than the former [28]. In addition, various extrinsic defects and impurities may further contribute to the dielectric constant and loss in the form of the Debye-type and Vogel–Fulcher–Tammann-type relaxations. The presence of porosity will bring a decrease in the effective dielectric constant of ceramics that can be quantified by the Maxwell–Garnett theory [29]. According to Fig. 10, the dependence of dielectric constant on the porosity of ceramics obeys the Maxwell–Garnett relation [30].

$$\varepsilon_{r,eff} = \varepsilon_{r,c}\left\{1 - \frac{3\phi(\varepsilon_{r,c} - \varepsilon_{r,d})}{2\varepsilon_{r,c} + \varepsilon_{r,d} + \phi(\varepsilon_{r,c} - \varepsilon_{r,d})}\right\}$$

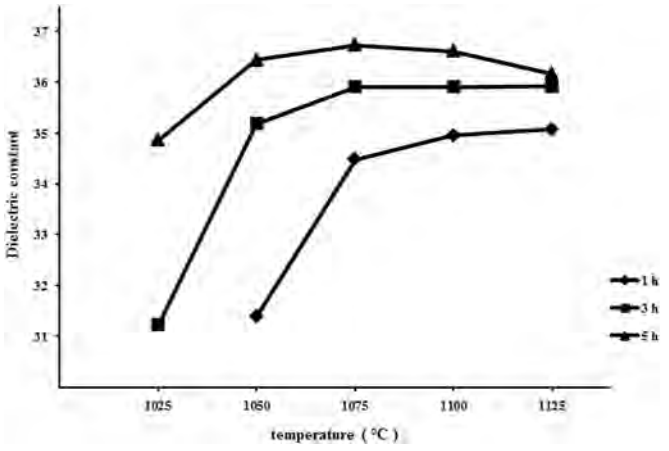

Fig. 9. Dielectric constant of ZTN ceramics against the sintering temperature and time.

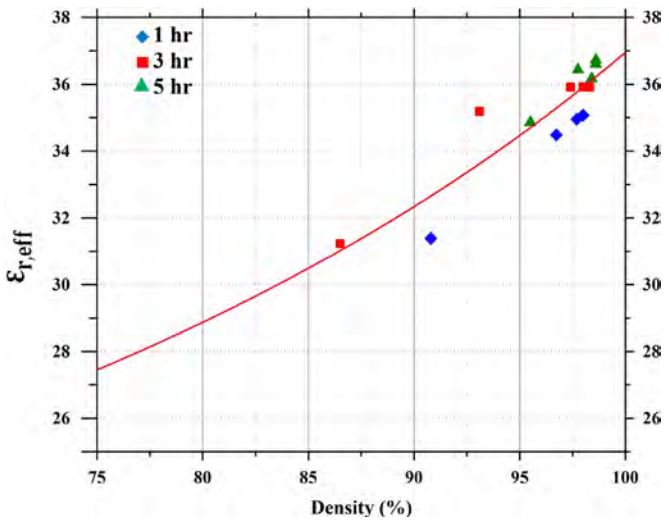

Fig. 10. Dependence of the dielectric constant on the density of ZTN samples. The line shows the Maxwell–Garnett fit to the experimental data.

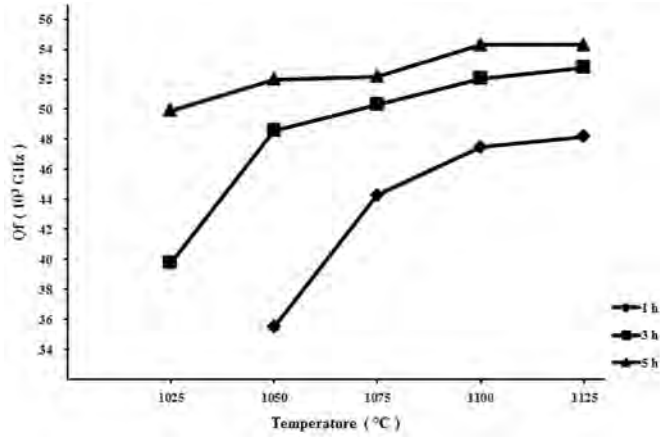

Fig. 11. $Q \times f$ values of ZTN ceramics against the sintering temperature and time.

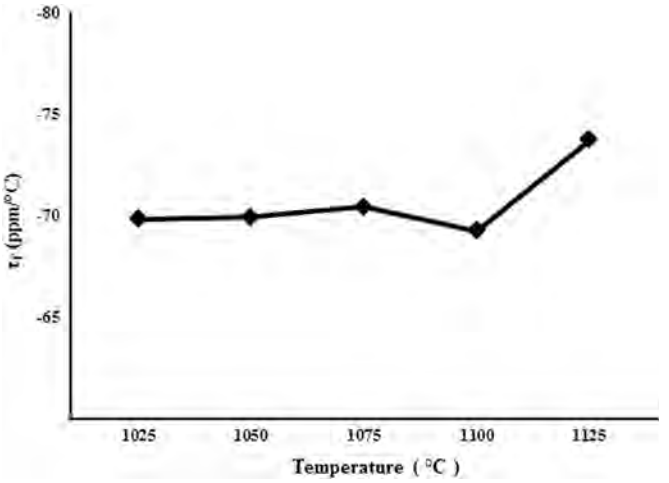

Fig. 12. Temperature coefficient of resonant frequency (τ_f) of ZTN ceramics sintered for 5 h against the sintering temperature.

where $\epsilon_{r,c} = 37$ for completely dense ZTN ceramics, $\epsilon_{r,d} = 1$ is the permittivity of vacuum, and ϕ is the porosity of ceramics. As expected, the effective dielectric constant of ZTN is dependent on the density of the samples. From Fig. 9, it can be observed that the trend between the ε_r values and sintering temperatures is similar with the trend between the densities and the sintering temperatures. A maximum ε_r value of 36.73 was obtained for ZTN ceramic sintered at 1075 °C for 5 h, which was similar with the results reported for ceramics obtained by the solid-state sintering method [5,9,10]. For example, Kim et al. [5] reported a dielectric constant of 34, Liao and Li [9] reported $\varepsilon_r = 34.4$ for ZTN ceramic sintered at 1120 °C for 6 h. Lei et al. [10] also reported that $ZnTiNb_2O_8$ sintered at 1150 °C exhibited the highest permittivity of $\varepsilon_r = 34.2$.

Fig. 11 shows the $Q \times f$ values of the ZTN ceramics. The microwave dielectric loss in ceramics is affected not only by the intrinsic dielectric loss due to the two- and three-phonon difference process [31], but also by the extrinsic losses such as the porosity, point defects, and second phase [32,33]. The variation of $Q \times f$ in ZTN ceramics show a similar trend with that of the relative density, which suggests that the dielectric loss is mainly controlled by the densification. Moreover, a maximum value of ~54,000 GHz could be achieved for specimen sintered at 1075 °C for 5 h, which was significantly higher than the results reported by the solid-state method [5,10]. By comparison, Kim et al. [5] reported a $Q \times f$ value of 33,000 GHz by the solid state technique. Lei et al. [10] reported that the ZTN ceramic shows the highest $Q \times f$ of 28,696 GHz.

Finally, Fig. 12 illustrates the temperature coefficient of the resonant frequency (τ_f) of ZTN ceramics. It has been known that the τ_f value is strongly dependent on the phase composition in the $ZnO–Nb_2O_5–TiO_2$ ternary field [6]. Since, in the present work the major composition and phase did not change with the sintering temperature, the τ_f values were not so sensitive to the sintering temperature. The values of τ_f in ZTN ceramics fluctuated around −70 ppm/°C with the increase in the sintering temperatures from 1025 °C to 1125 °C and these

values were ranged from −69.8 to −73.7 ppm/°C, similar with the results of other authors [5,9,10]. For example, Kim et al. [4,5] reported a τ_f value of −52 ppm/°C, Liao and Li [9] reported a slightly better value of $\tau_f = -47.94$ ppm/°C. Lei et al. [10] reported a very negative values of the $\tau_f = -75.84$ ppm/°C which are close to our results. On the other hand, Nenasheva et al. were able to achieve $\tau_f \approx 0$ ppm/°C in the two-phase ceramics consisting of the ixiolite and rutile phases [6].

4. Conclusion

$ZnTiNb_2O_8$ ceramics with pure ixiolite phase were obtained successfully by a reaction-sintering process. With increasing sintering temperature, the bulk density, ε_r and $Q \times f$ values increased; while the τ_f values changed only slightly. A density of 5.27 g/cm^3 (98.6% of the theoretical density) was obtained in $ZnTNb_2O_8$ after 5 h sintering at 1075 °C. Typically, $ZnTiNb_2O_8$ ceramics sintered by reaction-sintering method at 1075 °C for 5 h exhibited excellent combination of microwave dielectric properties such as, $\varepsilon_r = 36.73$, $Q \times f \approx 54{,}000$ GHz (at 6.7 GHz) and $\tau_f = -70.4$ ppm/°C.

Acknowlegements

T. K. was supported by Grant-in-Aid for Scientific Research C 26400323 from JSPS. Also, this work supported by "National Natural Science Foundation of China (U1232136)".

References

[1] I.M. Reaney, D. Iddles, Microwave dielectric ceramics for resonators and filters in mobile phone networks, J. Am. Ceram. Soc. 89 (2006) 2063–2072.
[2] T.A. Vanderah, Talking ceramics, Science 298 (2002) 1182–1184.
[3] W. Wersing, Microwave ceramics for resonators and filters, Curr. Opin. Solid State Mater. Sci. 1 (1996) 715–731.
[4] D.W. Kim, D.Y. Kim, K.S. Hong, Phase relations and microwave dielectric properties of $ZnNb_2O_6$–TiO_2, J. Mater. Res. 15 (2000) 1331–1335.
[5] D.W. Kim, H.B. Hong, K.S. Hong, Structural transition and microwave dielectric properties of $ZnNb_2O_6$–TiO_2 sintered at low temperatures, Jpn. Soc. Appl. Phys. 41 (2002) 1465–1469.
[6] E.A. Nenasheva, S.S. Redozubov, N.F. Kartenko, I.M. Gaidamaka, Microwave dielectric properties and structure of ZnO–Nb_2O_5–TiO_2 ceramics, J. Eur. Ceram. Soc. 31 (2011) 1097–1102.
[7] T.K. Chen, W.B. Ma, R. Li, Phase composition and microwave dielectric properties of (Zn, Ni)$TiNb_2O_8$ solid solution, J. Mater. Sci.- Mater. Electron 25 (2014) 2494–2500.
[8] Z.L. Huan, Q.C. Sun, W.B. Ma, L.J. Wang, Crystal structure and microwave dielectric properties of $(Zn_{1-x}Co_x)TiNb_2O_8$ ceramics, J. Alloy. Compd. 551 (2013) 630–635.
[9] Q.W. Liao, L.X. Li, Structural dependence of microwave dielectric properties of ixiolite structured $ZnTiNb_2O_8$ materials: crystal structure refinement and Raman spectra study, Dalton Trans. 41 (2012) 6963–6969.
[10] Y. Lei, Y.S. Yin, Y.C. Liu, Preparation and properties of $ZnTiNb_2O_8$ microwave dielectric cramics, Adv. Mater. Res. 217–218 (2011) 1235–1238.
[11] Q.J. Mei, C.Y. Li, J.D. Guo, H.T. Wu, Synthesis, characterization, and microwave dielectric properties of ixiolite-structure $ZnTiNb_2O_8$ ceramics through the aqueous sol–gel process, J. Alloy. Compd. 626 (2015) 217–222.
[12] A. Sayyadi-Shahraki, E. Taheri-Nassaj, H. Barzegar-Bafrooei, S. A. Hassanzadeh-Tabrizi, Microwave dielectric properties of $Li_2ZnTi_3O_8$ ceramics prepared by reaction-sintering process, J. Mater. Sci.: Mater. Electron. 25 (2014) 1117–1121.
[13] Y.C. Liou, C.T. Wu, K.H. Tseng, T.C. Chung, Synthesis of $BaTi_4O_9$ ceramics by reaction-sintering process, Mater. Res. Bull. 40 (2005) 1483–1489.
[14] Y.C. Liou, J.H. Chen, H.W. Wang, C.Y. Liu, Synthesis of $(Ba_xSr_{1-x})(Zn_{1/3}Nb_{2/3})O_3$ ceramics by reaction-sintering process and microstructure, Mater. Res. Bull. 41 (2006) 455–460.
[15] Y.C. Liou, M.H. Weng, J.H. Chen, H.Y. Lu, Synthesis of (Pb,Ca)$(Fe_{0.5}Nb_{0.5})_{1-x}Ti_xO_3$ ceramics by a reaction-sintering process, Mater. Chem. Phys. 97 (2006) 143–150.
[16] Y.C. Liou, W.H. Shiue, C.Y. Shih, Microwave ceramics $Ba_5Nb_4O_{15}$ and $Sr_5Nb_4O_{15}$ prepared by a reaction-sintering process, Mater. Sci. Eng. B 131 (2006) 142–146.
[17] Y.C. Liou, M.H. Weng, C.Y. Shiue, $CaNb_2O_6$ ceramics prepared by a reaction-sintering process, Mater. Sci. Eng. B 133 (2006) 14–19.
[18] Y.C. Liou, Y.L. Sung, Preparation of columbite $MgNb_2O_6$ and $ZnNb_2O_6$ ceramics by reaction-sintering, Ceram. Int. 34 (2008) 371–377.
[19] Y.C. Liou, S.L. Yang, Calcium doped $MgTiO_3$–$MgTi_2O_5$ ceramics prepared using a reaction-sintering process, Mater. Sci. Eng. B 142 (2007) 116–120.
[20] Y.C. Liou, W.C. Tsai, H.M. Chen, Low-temperature synthesis of $BiNbO_4$ ceramics using reaction-sintering process, Ceram. Int. 35 (2009) 2119–2122.
[21] Y.C. Liou, Z.S. Tsai, K.Z. Fung, C.Y. Liu, $Ni_4Nb_2O_9$ ceramics prepared by the reaction-sintering process, Ceram. Int. 36 (2010) 1887–1892.
[22] W.C. Tsai, Y.H. Liou, Y.C. Liou, Microwave dielectric properties of $MgAl_2O_4$–$CoAl_2O_4$ spinel compounds prepared by reaction-sintering process, Mater. Sci. Eng. B 177 (2012) 1133–1137.
[23] H. Barzegar Bafrooei, E. Taheri Nassaj, T. Ebadzadeh, C.F. Hu, Reaction sintering of nano-sized ZnO–Nb_2O_5 powder mixture: sintering, microstructure and microwave dielectric properties, J Mater Sci: Mater Electron 25 (2014) 1620–1626.
[24] J.H. Park, Y.J. Choi, S. Nahm, J.G. Park, Crystal structure and microwave dielectric properties of $ZnTi(Nb_{1-x}Ta_x)_2O_8$ ceramics, J. Alloy. Compd. 509 (2011) 6908–6912.
[25] D. Zhou, G. Dou, M. Guo, S. Gong, Low temperature sintering and microwave dielectric properties of $ZnTiNb_2O_8$ ceramics with BaCu(B_2O_5) additions, Mater. Chem. Phys. 130 (2011) 903–908.
[26] T. Kolodiazhnyi, Origin of extrinsic dielectric loss in 1:2 ordered, single-phase $BaMg_{1/3}Ta_{2/3}O_3$, J. Eur. Ceram. Soc. 34 (2014) 1741–1753.
[27] A. Baumgarte, R. Blachnik, Phase relations in the system titaniumdioxide-diniobium-zinc-hexoxide, Mat. Res. Bull. 27 (1992) 1287–1294.
[28] H. Froehlich, Theory of Dielectrics: Dielectric Constant and Dielectric Loss, 2nd ed, Oxford University Press, Oxford, UK, 1958.
[29] J.C.M. Garnett, Colors in metal glasses and metallic films, Philos. Trans. R. Soc., A 203 (1904) 385.
[30] M.M. Braun, L. Pilon, Effective optical properties of non-absorbing nanoporous thin films, Thin Solid Films 496 (2006) 505–514.
[31] V.L. Gurevich, A.K. Tagantsev, Intrinsic dielectric loss in crystals, Adv. Phys. 40 (1991) 719–767.
[32] J. Petzelt, N. Setter, Far infrared spectroscopy and origin of microwave losses in low-loss ceramics, Ferroelectrics 150 (1993) 89–102.
[33] T. Kolodiazhnyi, G. Annino, T. Shimada, Intrinsic limit of dielectric loss in several $Ba(B'_{1/3}B''_{2/3})O_3$ ceramics revealed by the whispering-gallery mode technique, Appl. Phys. Lett. 87 (2005) 212908.